CHAPTER-2

LITERATURE REVIEW

2.1 GENERAL

There are several developing countries that rely on nuclear energy to provide one fourth of the total electricity consumption. First nuclear plant APS-1 began providing commercial electricity power on 26 June 1954 at Obninsk, Russia. Double shell envelopes consisting of a primary internal steel containment or pre-stressed concrete shell and an external reinforced concrete shell are the majority of nuclear containment structures in the world. There are several different forms of nuclear power reactor in the world. Only the Pressurized and Boiling Water Reactors (PWR, BWR) are commercial in these days. Significant advancement of aircraft and missile technology has been gained by the twentieth century. When a NPP containment wall is subjected to aircraft crash, the material may get damaged due to high impact load and fire induced effects. So, the impact and fire related literatures have been discussed.

The aircraft impact can be defined as either soft or hard, depending mainly on the deformability of the projectile compared to that of the target. However, the aircraft's structure is made up of both components that are hard (stiffeners, landing gears, engines) as well as soft (fuselage) (Heckotter and Sievers, 2013). A RC building, like a containment of nuclear power plant can suffer flexural failure or bending due to an attack by soft missiles while punching shear failure or perforation due to a hard missiles attack. In addition to the specific mechanical properties of the ballistic projectile, a target's

failure mechanism often depends on its translational stiffness and impact velocity. The thick target is more vulnerable to shear failure whereas the slender target is more susceptible to flexural failure (Martin O., 2010). The available research studies in this field have been divided in two major categories according to the mode adopted for solving it. The two major categories are numerical studies and analytical studies. The research studies associated with the constitutive modeling of steel reinforcement and concrete and its behaviour are discussed separately under high strain rate and elevated temperature. On the basis of impact and fire effects on NPP containment wall due to aircraft crash, the existing literatures are divided into three main categories. The categories are given below:

1. Analytical approach
2. Numerical approach
3. Material behaviour under impact and fire

2.2 ANALYTICAL APPROACHES ON NPP CONTAINMENT WALL

When the aircraft breaks contact with the structure, the impact load is converted into an impulse load. In this area, the work performed by Riera (1968) to uncouple the aircraft crash issue is considered to be the benchmark. Using the aircraft's inertial and stiffness characteristics, the total reaction of the Boeing 707-320 against a rigid target over time was obtained. In the measurement, an impact velocity of 102.8 meter/sec was assumed and the angle of impact was assumed perpendicular on the target. If the aircraft is going at a constant rate, the momentum is directly proportional to the initial velocity and the total mass. The aircraft’s momentum M(t)V(t) is governed by the mass and the initial velocity of the aircraft. The overall reaction F(t) at the interface between

the collapsing aircraft and the rigid body is determined by applying some justified assumptions to the principles of momentum conservation (Fig. 2.1). An aircraft's impact force is represented by the following equation namely the Riera function:

$$F(t) = \frac{d}{dt}[M(t)V(t)] = M(t)\frac{d}{dt}[V(t)] + V(t)\frac{d}{dt}[M(t)] \qquad (2.1)$$

$$F(t) = M(t)a(t) + V(t)\mu_1[x(t)]V(t) = P[x(t)] + \mu_1[x(t)]V^2(t) \qquad (2.2)$$

Where-

$V(t)$	Velocity of aircraft at time t
P[x(t)]	The aircraft's crushing strength
$\mu_1[x(t)]$	Longitudinal mass distribution
$\mu_1[x(t)]V^2(t)$	Inertial force
$M(t)$	Mass of aircraft at time t
$M(t)V(t)$	Momentum of the aircraft
$F(t)$	Obtained reaction force from target

From above Equation, it can be noted that the aircraft's crushing strength and mass density depends specifically on both x (distance) and t. (Time). The linear mass density and crushing strength of aircraft vary with its length, Riera (1968). In Riera equation, only the mass distribution, initial velocity and the crushing strength are necessary, as shown in equation 2.2. Then a numerical step-by-step method can be built to measure the impact force-time history using the fundamental kinematic relationships (Lee et al., 2013).

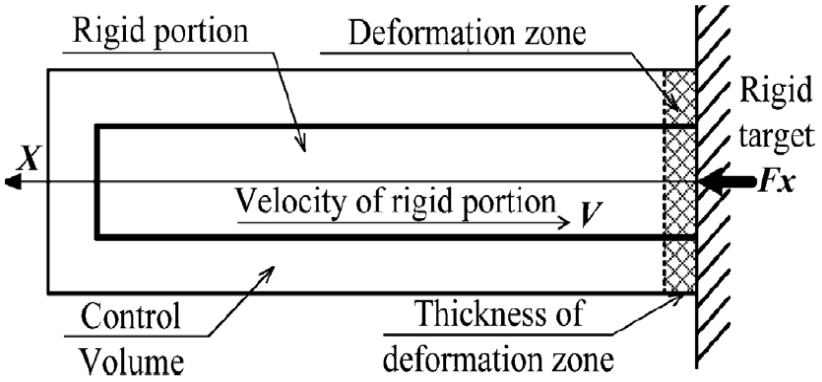

Fig. 2.1 Riera's aircraft impact model (Riera, 1968)

Rice and Bahar proposed an alternate derivation to obtain the reaction-time response curve (1978). The disadvantage in this derivation is the assumption that in the control volume, the distribution of velocity is constant. Due to the assumption that the deformation region is mathematically zero, there will be a finite jump in velocity at the projectile-target interface. In fact, relative to the total un-deformed volume, the thickness of the deformation zone is negligible, but not mathematically zero. In an attempt to improve the formulation of the Riera, Hornyik (1977) determined the energy balance with the assumption of the projectile's rigid, fully plastic behaviour. Wolf et al. (1978) used lumped masses intertwined by elasto-plastic springs as the aircraft model in another compression analysis to determine the reaction-time curve of the Riera. The authors find that the two models agree exceptionally well for a number of impact velocities.

Damping is ignored during the containment analysis through the application of the force-history curve, as it does not affect the full impact loading response (Rebora et. al., 1976). The influence of gravitational forces on the reaction was found to be negligible, and stresses due to gravity were also very small (Gardner, 1984 and Abbas, 1992). The elastic stiffness of the aircraft body does not play a major role in the reaction time curve

for soft projectiles, such as airplanes flying at normal velocity. An accurate assessment of buckling behaviour and crushing strength, however, is of great significance (Bignon and Riera, 1980). Riera et al. (1982) stated that engines should be treated as separate projectiles in the event of an aircraft impact on nuclear structures and, if possible, their influence should be added on the fuselage. An attempt to enhance the design of the containment was made in order to survive in this abnormal situation. Paul, et al. (1993) analysed the effects of the Boeing 707-320 aircrafts at three different positions of a boiling water reactor containment house (Fig. 2.2). It was concluded that the 1.2 m thick cylindrical wall and 0.61 m thick dome are adequate to withstand the horizontal crash near the dome and cylinder junction, but may be dangerous for any other locations.

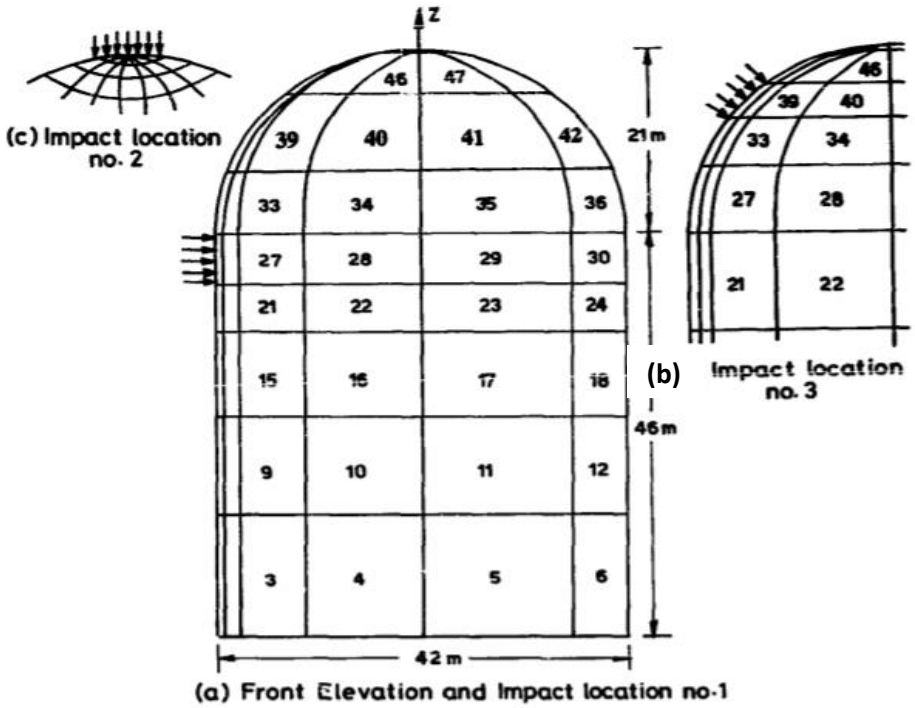

Fig. 2.2 Impact location on NPP containment (Paul et al., 1993)

Zerna et al. (1976) proposed that for aircraft-impact resistant structures, steel fibers and cables could allow new design solutions. Steel fibers and cables which are used

to strengthen the structures would allow for more structure deflection than was originally allowed. The thickness of the containment can therefore be reduced because it only offers penetration safety and is independent of the shear and bending requirements. In addition, Krutzik (1988) proposed that steel-fiber-reinforced concrete structures with thicknesses equal to or greater than 0.8 m have adequate nonlinear potential to withstand a military aircraft crash such as the Phantom plane. Koechlin and Potapov (2009) concluded in a latest study that an aircraft crash is a soft impact and that it would be a shear cone failure mode if perforation occurs. The influence of the target yield was also analysed in some available literatures and led to the conclusion that the flexibility of the target does not have a major effect on the curves of reaction time (Riera, 1980, Drittler et. al.,1977, Wolf et al., 1978, Nabold and Schildknecht, 1977). On the other hand, Abbas et al (1995) found that not only unrealistic but also un-conservative is the reaction time response obtained on the basis of a rigid target. It was also observed that the effect of the target yield depends on both the target and the missile characteristics. Therefore, using the reaction-time response obtained on the basis of a rigid target concept is impractical. This is a new finding that the author of this thesis has reached. While Abbas et al (1995) commented on the target yield, they were unable to obtain any significant effect of the target yield on the Phantom F4, FB-111 Fighter Jet and Boeing 707-320 aircraft reaction time response. The reaction time response of various fighter and commercial aircraft based on Riera's approach was subsequently suggested by several researchers (Gomathinayagam et al., 1994, Abbas et al., 1995&1996, Iliev et al., 2011, Lo Forano and Forasassi, 2011). A few aircraft have been provided with reaction time response curves in Fig. 2.3 in order to compare. It can be observed that current commercial aircraft may have higher impact force and, due to their huge length and high crushing strength, their impact period is also longer.

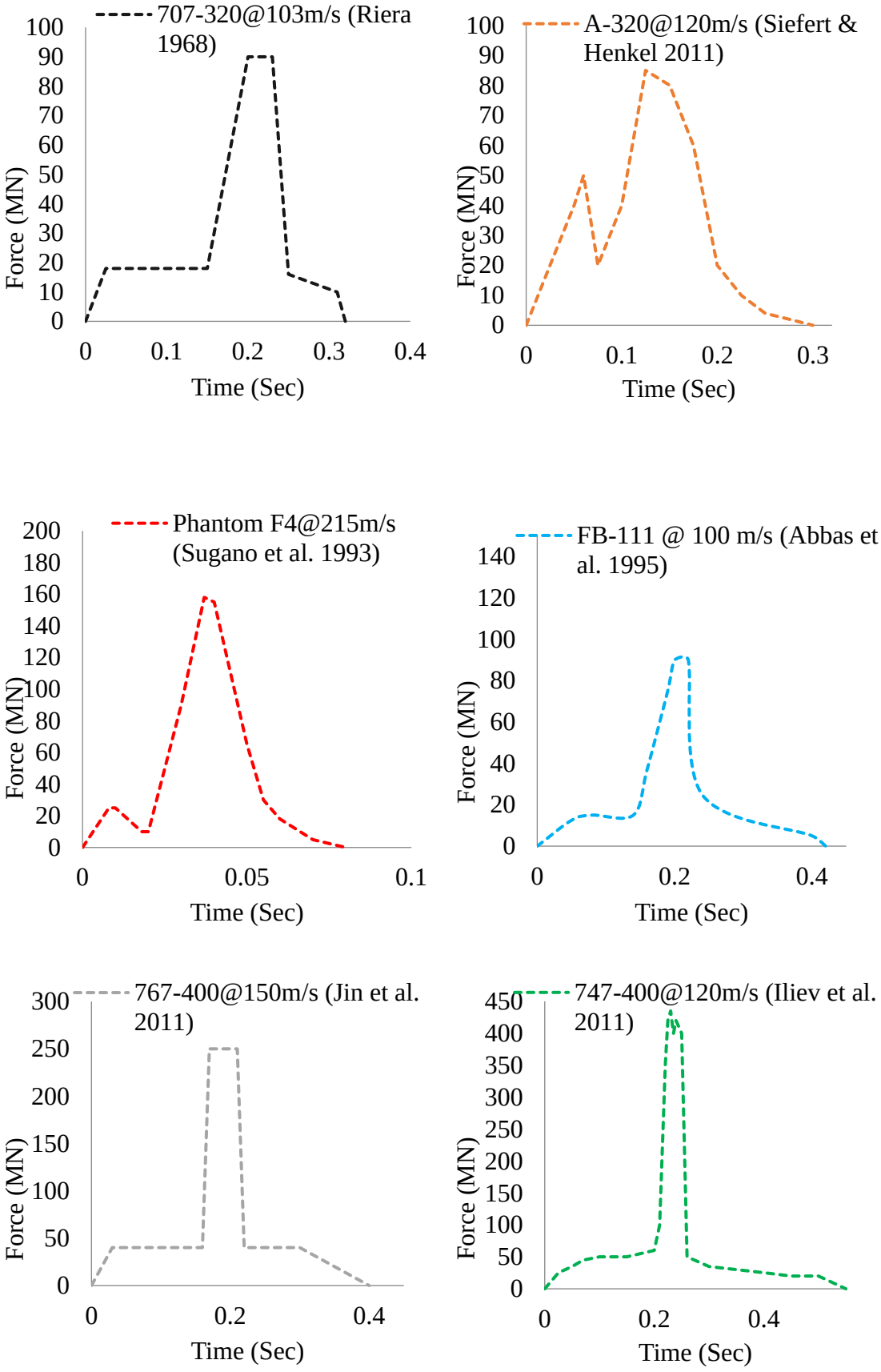

Fig. 2.3 Different aircraft reaction time response curves

Experimentation with this issue is extremely costly, challenging and dangerous, such that such studies can be almost impossible for individuals and academic institutions to conduct. Despite this, however, Sugano et al. (1993) performed one experiment in which the Phantom F-4 fighter jet crashed on a thick concrete wall at the Sandiya laboratory, USA. A full-scale aircraft impact test was performed by Sugano et al. (1993) against a thick, reinforced concrete target. The overall weight of the aircraft, along with the weight of the attachments and 4350 kg of water that was filled to simulate the fuel and achieve mass distribution, was 17000 kg. The target made up of a horizontal and vertical reinforced concrete wall with a span of 7 m with 3.66 m thickness. In relation to the target, the orientation of the aircraft was considered normal while the velocity of incidence was 215 m/s (Fig. 2.4).

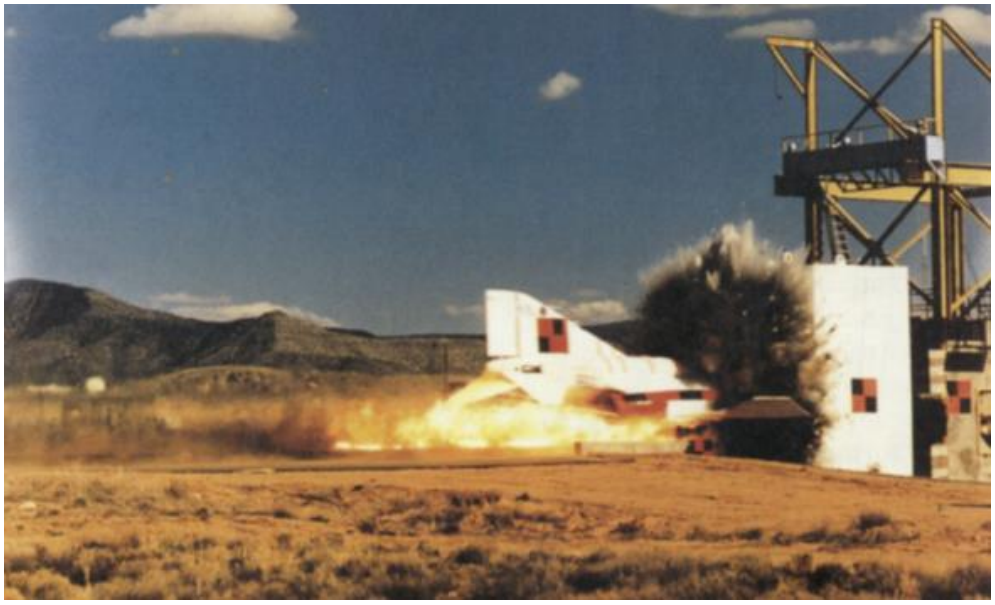

Fig. 2.4 The aircraft's view during impact (Sugano et al., 1993)

The maximum concrete penetration caused by the engines was 60 mm, and 20 mm was caused by the fuselage. The RCC wall experienced a 1.83 m displacement and

rebounded back against the back-up structure. The sensors were placed on the aircraft and the target for kinematic measurements. The cumulative impact force (F) was calculated independently of the change in the momentum of the target and aircraft. The experimental data suggested that the existing "Riera approach" can be used to evaluate the impact force for different aircrafts. The authors systematically executed the impact of engines separately, motivated by a full-scale aircraft impact test. As they noted during in the full-scale test, the engines in the massive concrete target caused deeper local penetration than the aircraft fuselage. In addition to full-scale tests, an extensive series of engine impact tests were carried out on scales 1:2.5 and 1:7.5 in order to determine low-cost feasible testing patterns. This important result allowed researchers to enhance their investigation of varying parameters in aircraft impact studies to small testing facilities in laboratories.

Riedel et al (2010) have reviewed an experimental series on Ultra High-Performance Concrete (UHPC) panels subjected to aircraft engine impact with comparison to a test series on standard strength concrete. A small-scale model of the laboratory was developed and the testing was carried out at a scale factor of 1/10. The Ultra High-Performance Concrete is a concrete-based material that integrates ultra-high strength, high density of packaging and enhanced ductility. Owing to the presence of fiber reinforcement, it also possesses substantial energy dissipation ability. The above characteristics restored the depth of penetration to a mere footprint and controlled concrete spalling. The fibers stayed attached on the rear side of the concrete panel until the width of the crack equals half of its length and thus prevented scabbing of the matrix.

Farmer (1967) and Wall (1969) also suggested probabilistic approaches to the design and safety study of nuclear power plants. They set a boundary line that

distinguishes between acceptable and unacceptable risks. The normal procedure before the WTC attack in September 2011 was to assess the risk of an aircraft accident at a nuclear power plant. The chance of an impact was ignored as the design basis criterion if the probability was calculated to be less than a specified permissible limit. Necessary steps were otherwise taken to minimize the risk of general strike. The absolute and conditional probability of failure of the RC concrete walls of the nuclear power plant due to an aircraft accidental strike was calculated by Chelapati and Kennedy (1972). It has been shown that the response of the entire building is negligible if an aircraft hits a reactor building, but severe damage takes place to its particular structural elements. In order to assess the conditional probability of local collapse of the wall panel, the probabilistic methods and yield line theory were used. It was reached the conclusion that the probability of damage was approximately the same order of magnitude under the perforation and collapse mode. The cracking mode of damages was estimated using elastic analysis under the impact of an aircraft. The cracking mode of damage has been predicted to occur much faster than the other 2 damage modes i.e., collapse and perforation. The pattern of impact load predicted for the cracking mode of damage has also been shown to be very conservative. The accident probability on the plant site by a military aircraft on a racetrack pattern flight was evaluated by Hornyik et al. (1973). The possibility of an accident on a NPP plant near the flight region was investigated by Zorn and Schueller (1986) Kobayashi (1988), assuming that the flight density in the area and also the direction of flying is uniform. Zorn and Schueller (1986) noted that the engines detached from the fuselage shortly after impact, following a detailed analysis of aircraft crash incidents. The superposition of the heavy engine and the effect of the soft fuselage was emphasized as a time and spatial problem where the geometry of the target should not be avoided. Siddiqui et al (2003) found in a reliability analysis that with the increase

in takeoff point distance from NPP, the reliability of containment increases dramatically. The rate of increase in reliability, however, slows down as the distance gets longer. The mass and velocity of aircraft have been found to have a remarkable impact on the reliability of NPP containment. For other aircraft with the same speed but higher mass, a containment that is effective against one aircraft strike may be highly unreliable. In short, it should be remembered that the accidental crash affects most probabilistic research. In recent years, however, the vulnerability to intentional attacks has been shown to increase significantly.

2.3 NUMERICAL APPROACHES ON NPP CONTAINMENT WALL

A non-linear simulation of model requiring many time steps to determine the impact response includes analysis of nuclear containment structures against aircraft impact (Gomathinayagam et al., 1994). Using high speed computing facilities and advanced finite element codes, non-linear finite element analysis of aircraft crashes on essential concrete structures such as nuclear containments and military installations has been studied.

Abbas et al. (1995, 1996) concluded that the most vulnerable zone is the junction of dome and cylinder, and Boeing 707-320 and FB-111 jet fighter is less damaging than Phantom F4. Using the AUTODYN-3D computer software, Katayama et al. (2004) carried out a 3-dimensional computer simulation of the impact of a Boeing 747 passenger jet. RC and non-RC concrete walls of three different thicknesses were the targets. It was observed that when impacted by the aircraft at 300 km/h impact velocity, the reinforced concrete of 3 m thickness was not seriously affected. However, the assumption

introduced in Katayama (2004) needs to be checked in order to enhance the accuracy of the simulation. For example, because of the lack of knowledge about its exact position, the weight of the fuel was distributed equally to all elements of the jetliner.

To compare the response of a hypothetical nuclear structure, Arros and Doumbalski (2007) used the reaction-time curve as well as the geometric Boeing 747-400 aircraft model. The Boeing-747 numerical model was designed with wing load spread throughout the total length. It was also observed that if the area of the wing is marginally decreased, the displacement obtained by the curve of reaction time would match exactly that of the geometric model. Kukreja (2005) identified that by experiencing local damage and perforation, the outer layer of BWR Mark III and PHWR containments will absorb significant energy from Boeing 707-320 and Airbus 300B4, while the inner layer will undergo negligible deformation. Lo Frano and Forasassi (2011) noticed that when impacted on IRIS containment buildings, Boeing-747 has the highest damaging capacity (with 1.0 m penetration depth), followed by Boeing-707, Boeing-720 and Phantom F4. If the containment layer is less than one-meter thick, serious damage may take place to commercial aircrafts.

Almost all of the numerical studies were carried out with some method of finite element analysis. The finite element technique is highly flexible and efficient, enabling the correct use of this technique to solve incredibly advanced scenarios. The performance of the simulation of the finite element depends on different variables, such as the method of analysis, the size of the increment, the conditions of contact and boundary, the size of the element and its aspect ratio. The element size of the model depends on the issue and the particular outcomes that need to be achieved. The mesh convergence analysis must

therefore be conducted in order to obtain reliable results via a finite element simulation. To discretize the BWR containment, Abbas et al. (1996) adopted 20-noded isoparametric brick elements with a total number of 342 nodes. Kukreja (2005) considered a few hundred elements and after that Iqbal et. Al., (2012) used a total of 514,640 elements for the similar simulation in the containment. In their results, the influence of element size is clearly evident. The deformation (depth of maximum penetration) of the containment found at the dome and cylinder junction by Abbas et al. (1996) was 34.2 mm, while Kukreja (2005) verified his material model with Abbas et al. (1996) and stated that at the same location the maximum deformation was 46 mm. Therefore, at the same place, Iqbal et al. (2012) found a maximum deformation of 66.9 mm. Ciria et al. (2008) stated in another analysis on a cantilever beam in the condition of plane stress that relative error was reduced from 10.5 percent to 0.066 percent with an increase in the total number of elements from 34 to 5506. It can therefore be observed that an optimal element size must be carefully chosen for all regions of highly concentrated stress, such as around loading points and supports, taking into account the precision of the solution and the availability of the computer setup.

There are two simple methods to the computational simulation of the aircraft crash problem related to the application of load, i.e., either to model the aircraft geometry to reach the target structure or to apply its loading via the response time response curve. In a finite element code, the development of an accurate geometric aircraft model and its discretization is very complex. With nonlinear geometry and varying stiffness, the new commercial aircraft have complex structures. The fuselage of an aircraft is a permanent structure in which aluminium alloy skin keeps up cabin pressures and stresses. For resisting longitudinal tension and compression, longitudinal stringer is required.

Circumferential frames are employed to retain the fuselage shape and disperse the skin load. Thick bulkheads are used in place of frames for regular military aircraft (Starke Jr. and Staley, 1996). It is important to pick a proper constitutive model and characterize the material. It is also necessary to determine an equivalent stiffness for the fuselage, wings and intermediate stiffeners. The thickness of wings varies from the joining point of the fuselage to the extreme wing section. Therefore, it is almost difficult to prepare a geometric model that replicates all the characteristics of an aircraft identically.

Elsewhere, it is the impact area that should be accurately determined along with the reaction time curve in the reaction time response strategy. Riera (1968) took a schematic approach to measure the probable interface between a Boeing 707-320 aircraft on crush normally on a spherical surface of diameter 67 m. It was found that the area of impact may be calculated to be 20.43 m^2 if the impact is considered at the dome, whereas it could be about 37.16 m^2 for a flat surface. Yang and Godfrey (1970) suggested in another study that the interface region between the structure and aircraft would be about 10 to 15 percent more than the aircraft's cross-sectional area.

Riera (1980) assumed the impact area to be 7 m^2 for the strike of the Phantom F4 on a rigid target. On the other hand, through experiments, Sugano et al. (1993a) found that the estimated fuselage area was 4.6 m^2, while the area of impact was 10 m^2 against a flat concrete target. It should be indicated that it was considered that the area of impact was roughly circular and that the effect of the wings was ignored (Fig. 2.5). In addition, Abbas et al (1995, 1996) considered an area of effect of 28 m^2 for Boeing 707-320, Phantom F4 and FB 111 aircraft affecting the 42 m diameter containment of the BWR Nuclear Power Plant. The impact area for all the aircraft considered in his analysis was

also assumed to be 28 m2 by Gomathinayagam et al. (1994) and Kukreja (2005). While researching the impact of the Boeing 747-400, Aross and Doumbalski (2007) stated that the outcome of the Riera time history approach could be very sensitive to the assumptions correlated with the loading area and load application timing. Iliev, et al. (2011) considered the area of impact to be circular, 8 m in diameter, for aircraft Boeing 747-400 while the wing area to be rectangular, 33 m × 2 m. Jin et al. (2011) segregated the fuselage and wing impact area for the Boeing 767-400 and noted that the engine contributes primarily to the overall impact load. The reaction time curve of the engines, wings and fuselage was applied separately by Siefert and Henkel (2011) to their corresponding contact area measured by the authors. It was found that the load-time-function shows the lowest displacement values for the simulation of an Airbus A320 than for the geometric model based. This confirms the common assumption that the load-time-function findings are typically conservative.

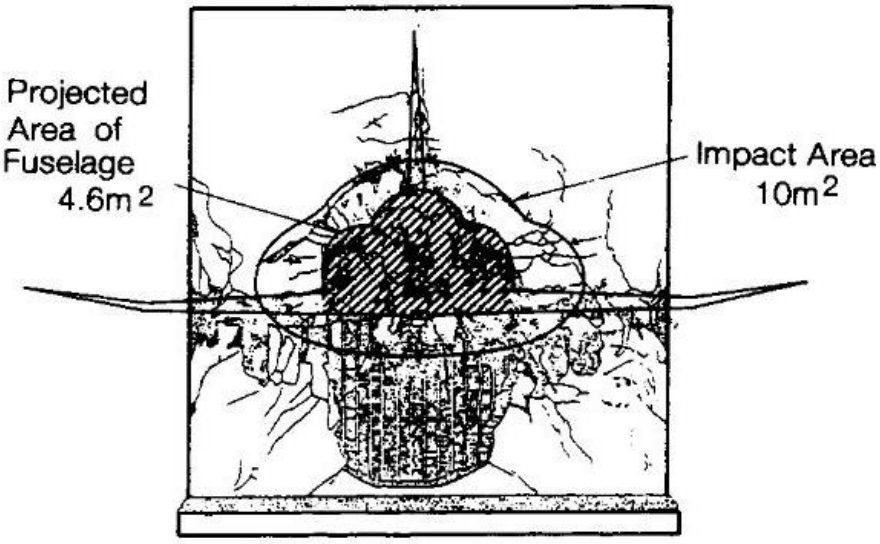

Fig. 2.5 Impact Area (Sugano et al., 1993)

It is not possible to achieve a precise demarcation of the impact region for the aircraft's fuselage, engines or wings and its corresponding reaction curve, as the effect of one part of the aircraft on the force reaction curve of the other part cannot be ignored. Therefore, the issue of an effective impact area requires further study in order to create a standard design code.

The force due to aircraft impact can be calculated on the nuclear power plants containment structure by assuming it as a rigid body or an elastomer (Yan and Liu, 2015). Therefore, the approach proposed by Riera can be effectively used to determine the overall load of the impact with respect to time. The distribution of the load could not, however, be calculated by this method. As a consequence of nonlinear models and uniform body surface loading, there are significant variations. The load distribution therefore needs further analysis.

Sang-Shup Shin (2015) used a finite element approach and smooth particle hydrodynamic (SPH) technique to create an aircraft model including jet fuel. Compared to the impact test results of aluminium cylinder fluid projectiles, the SPH model for jet fuel is verified and the simulation process was adapted to the specification of the aircraft model. After impacting the reactor containment building wall, the aircraft-structure interaction analysis was carried out to determine the dispersion region of jet fuel on the auxiliary building roof area, and this study proposes the fire curve for heat transfer and stress analysis. Finally, under the fire curve, the structural integrity of the auxiliary building roof was evaluated.

The structural integrity of a reinforced concrete containment vessel (RCCV) against the direct impact of Phantom F4, Boeing 707-320 and Airbus A320aircraft was investigated (Reza Saberi et al., 2017). The 3D numerical simulations were carried out using the finite element analysis solver software (ABAQUS/explicit). The impact positions defined on the structure of the NPP containment are mid containment height, center of the cylindrical section, dome and cylinder junction, and near the foundation level over the cylindrical portion. The aircraft loading was allocated via the corresponding reaction time response curve. The CDP model was projected to simulate the concrete behaviour while the elastoplastic material model was used to integrate the behaviour of steel reinforcement. Using the dynamic modification factor, dynamic loading conditions were considered. For each aircraft crash, the mid containment height and middle of the cylindrical section have been found to undergo the most extreme deformation. In concrete, serious damage cannot be expected by the impact of considering aircrafts.

The study of the stress-state measurement results of the aircraft impact NPP structures was conducted on the basis of formulated strength and failure survival requirements for reinforced concrete structures (Fedorenko R. V. et al., 2017). Using the parametric simulation model, the optimum value of the thickness of containment can be calculated and, overall, the influence of this parameter on the outcome of the impact of the aircraft can be investigated. It was determined that dynamic loads on secondary systems significantly depend on the locations and heights of target points. In reality, values of acceleration can exceed several tens of gravities. However, the thickness of the outer containment has no direct relationship on the maximum values of accelerograms.

Thus, it is important to solve the problem of reliability of secondary systems during the design of the NPP structures in order to solve the general structural strength problem.

Sadique et al. (2018) performed the heat transfer analysis on a flat RCC plate using Boeing 707-320 aircraft. The maximum temperature in concrete body was observed about 974oC. The material properties for concrete and steel reinforcement were taken from Euro code-2. The time duration for impact was considered up to 0.016 sec. For heat transfer analysis, two fuel curves for different region were applied.

The commercial aircraft Boeing 767-200ER was applied on NPP containment structure wall to get the response using geometric model of aircraft (Xiaoxin Wang et al., 2019). Two different aircrafts were considered. The reaction force-time curve obtained by the FEA tool was compared with Riera function which was proposed in 1968. The mesh sensitivity of NPP containment model was analysed and some recommendations on the modeling of containment were given. The damages due to aircraft crash on the NPP containment were studied. The fuel capacity of the aircraft was found to have a strong effect on the damage of containment wall. It was also suggested that the load distribution in the transverse direction was important in the analysis of aircraft impact.

2.4 CONCRETE AND STEEL BEHAVIOR UNDER HIGH RATE OF LOADING AND ELEVATED TEMPERATURE

The concrete’s dynamic behavior depends on the boundary conditions or confining pressure and is significantly non-linearKalpan's (1961) thesis on the fracture mechanics of concrete has continued for more than half a century. Hao and Hao have

published the most recent study on this subject (2013). Kesler et al. (1971), Walsh (1972), Hillerborg et al. (1976), Hillerborg (1985), Bazant and Cedolin (1991) made a substantial contribution to the development of fracture mechanics of concrete.

Many variables, such as conditions of impact, geometry and material parameters control the failure of a target structure. A clear understanding of strain softening and fracture energy behavior will predict the failure of the concrete target. Fracture energy can be described as the energy needed to remove the crack surface area of a unit. Initially invented by Hillerborg et al. (1976), the fictitious crack model (FCM) is an efficient mechanism for predicting crack growth in concrete. fracture energy is a special material property that is not dependent of type of loading, specimen size, and shape (Bazant and Pfeiffer, 1987). For fracture energies, an approximate selection of specimen sizes was discussed but the accurate range of specimen size was still unknownHowever, large specimens need to be checked to measure a size-independent fracture energy value (Muralidhara et al., 2013)

The reinforced concrete target's failure mechanism affected by a projectile would be either shear dominant or flexure dominant. Both of these are the consequences of the growing problem of being damaged. The reinforced concrete target was found to have elastic and plastic modes of failure. In the case of a flexural failure, stress is applied to the front surface of the target and tension is applied to the distal surface. This situation contributes to the development of fractures along the target thickness. Therefore, the cracking strain was identified as a sensitive parameter by Abbas et al. (2004), so it needs precise assessment for accurate analysis purposes. A shear cone forms inside the target in the moment of puncturing shear failure. In the worst-case scenario, the shear cone is

punched out of the concrete target. In comparison to the flexural failure in which the compression/tension is predominant, the material fails because of excessive shear stresses (Martin, 2010).

Failure modes sometimes depend on the concrete strength, the amount of reinforcement and projectile shape. The target made up of over-reinforced concrete is vulnerable to flexural failure, as is the target subjected to low velocity impact or soft impact. On the other hand, it is more likely that the under-reinforced target and the target subjected to a hard impact or high velocity impact will experience punching failure. The reinforcement spacing and the diameter of the projectile can also have an effect on the process of failure.

The concrete failure mechanisms such as penetration, perforation, cone cracking, spalling and radial cracking were defined in detail by Li et al. (2005), Fig. 2.6. The punching failure was subdivided into four separate types of local failure, i.e., surfaces failure, perforation, spalling and scabbing:

- Penetration is characterized by the projectile as tunneling into the concrete target. The tunnel length is considered the depth of penetration.
- The word "cone crack and plugging" refers to the creation of a cone-like crack under the projectile and the resulting shear plugging.
- Spalling happens when the proximal face of the target material has been shattered off by the projectile.
- The concept of Radial Cracking is the propagation of cracking from the impact point towards the proximal or distal face or both.
- Scabbing is exactly the elimination of fragments on the back of the target.

- Perforation is when the projectile passes through completely without leaving residual velocity.

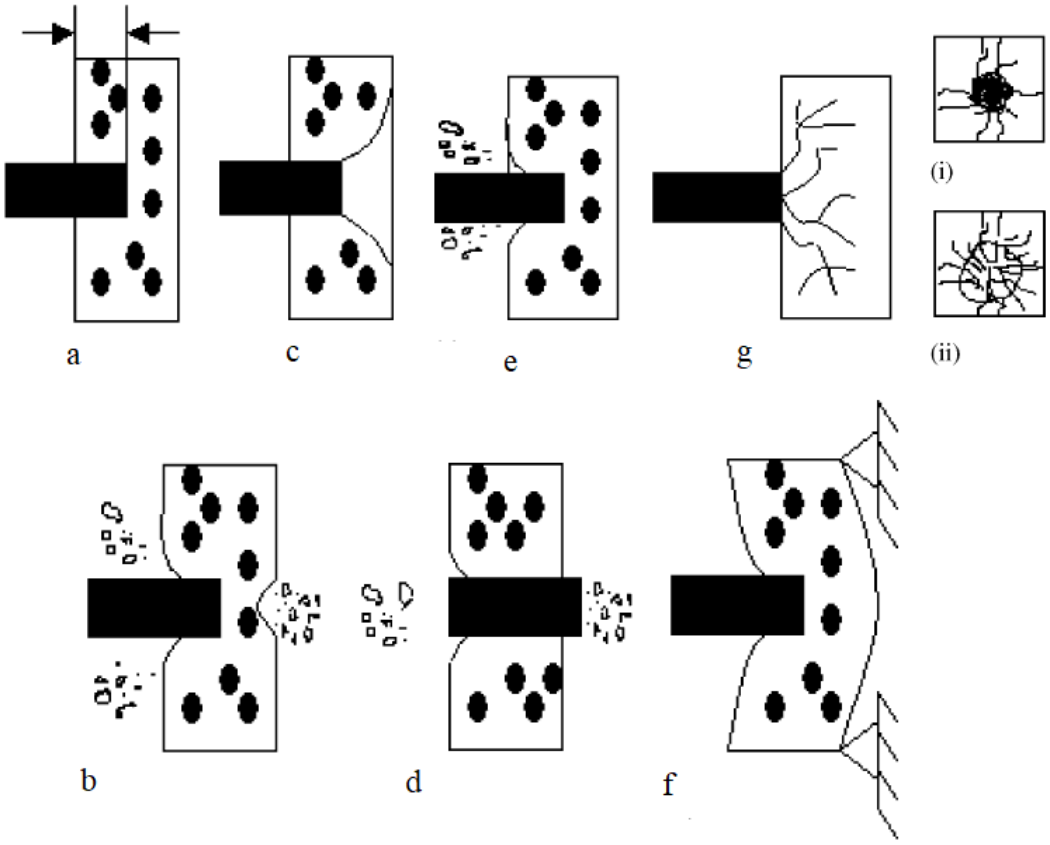

Fig. 2.6 Brittle target subjected to projectile impact (a) Penetration (b) Scabbing (c) Cone cracking (d) Perforation (e) Spalling (f) Overall target response (g) cracks on (i) front face (ii) rear face (Li et al., 2005)

The cause of local punching for the target/projectile scenario is usually the thickness to projectile diameter ratio (x/d) and the stress wave characteristics of the structure. If the target is very thick, and the velocity of the projectile is small, then there is sufficient resistance and the damage is restricted to the surface. However, if the velocity of projectile is greater, the projectile will produce a cone-like pit on the projectile's front end and material from the front will be expelled. This is a recognised technical term

called spalling. If the x/d ratio is small and the projectile velocity is large, there are huge shock waves produced on the rear surface surface of the target (not the projectile itself). These waves effect the material from the rear surface and knock it out. This is known as 'scabbing'.

Too many different mathematical models have been developed in order to predict behaviour of concrete structures under massive loads. Some few fracture models were studied for high-dynamic simulation of concrete structures by Wierzbicki et al., in 2005 and Lu and Tu in 2009. Researchers concluded that the "damage model" is able to simulate concrete behaviour under a wide variety of stress conditions. However, no single material modeling method can simultaneously model the impact, shock blast or fire precisely at the same time (Lu Y., 2009).

Concrete is a much-used material in building and is usually fire resistant. concrete has good fire-retardant qualities. Other than being non-combustible, non-smoke generating and not dripping liquid, it also remains non-corrosive. The key aspect of the design requirements is, in general, the sufficient reinforcement cover. A typical laboratory setting is significantly different from a real-world scenario. The cooling process of an extreme fire is different from each other, but the initial heating rates may not be the same. The behaviour of concrete material under fire is entirely dependent on the material's temperature-dependent properties. The strength and elastic properties of concrete decrease with an increase in temperature and at the same time the material expansion contributes to the creation of stresses in the materials in addition to the stresses formed due to loads. At high temperature, concrete decreases its strength and depending on the type of aggregate used. The three primary aggregates used are carbonate, silica

and lightweight aggregate. Dolomite and Limestone fall under carbonate aggregates whereas sandstone and granite fall under siliceous aggregate. Light weight aggregates are usually produced after thermal treatment of shale, slate, or clay.

The literature on the elevated temperature behaviour of concrete can be roughly divided into three parts;

- Studies are based on fire duration and its intensity
- As a concrete continues to get hotter, its thermal and mechanical properties change
- Fire has a big effect on structure and its elements

The degradation of cementitious materials due to exposure to high temperatures can be classified as types as below.

- Phase transition occurring in cement paste. (Malhotra 1956, Khoury 2000).
- Concrete Spalling (Khoury and Adenburg, 2000).
- Phase transformation that takes place in aggregate (Fletcher et al 2007),
- Thermal variation between the paste of aggregate and cement (Fletcher et al., 2007),

However, Usmani et al. (2001) clarified that instead of material degradation, the structural change in fire is more governed by the induced stresses and displacements. The interface illustrations for structure parts at ambient and elevated temperatures were also proposed by Law and Gillie (2010). The influence of fire on RCC structures during the heating process is shown in Table 2.1. Based on the fact that the optimum temperature in material is reached during the cooling process, the cooling phase is assumed equally

significant. Therefore, during the cooling process, the structural elements are more vulnerable to failure. Fig. 2 .7 demonstrates the different form in concrete surface texture when exposed to elevated temperatures of up to 1200 ^{0}C, (Omer, 2007).

Table 2.1 Various stages of heating phase

Heating stage	Probable effects
Surface temperature increase	Cracking of surfaces
Transferring heat from the outside to the concrete interior	Strength loss, starts cracking and spalling
Transferring heat from concrete to reinforcement	Reduction in strength, increases in buckling and deflection.

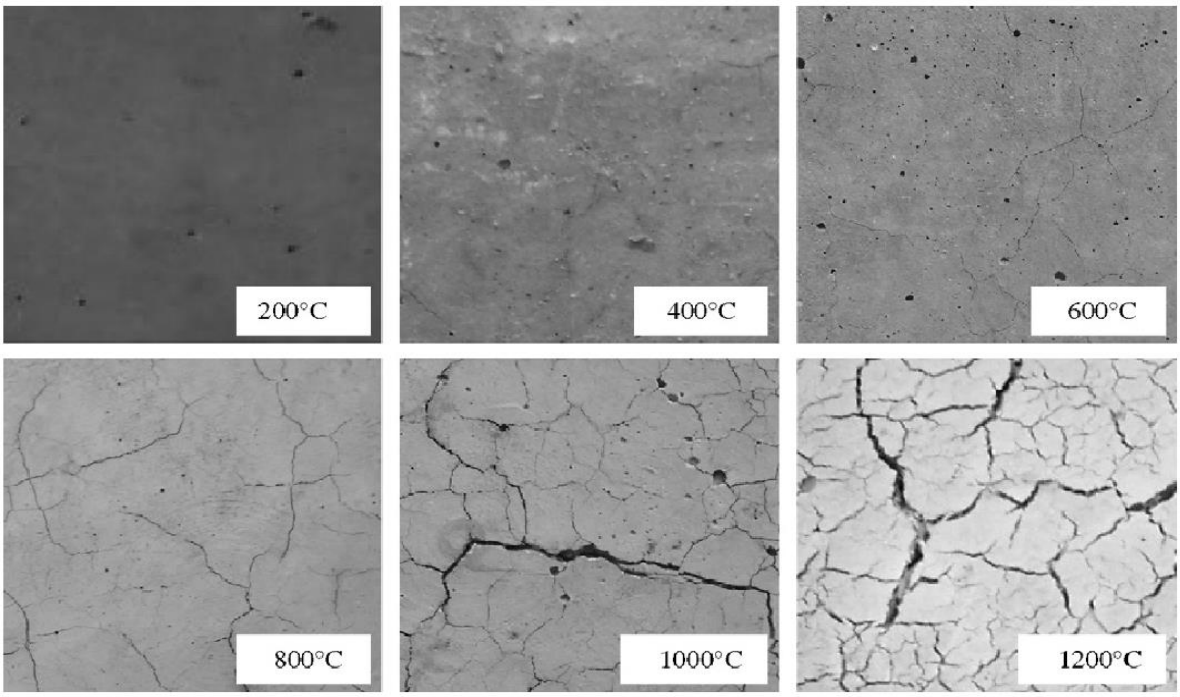

Fig. 2.7 Different form of surface texture of the concrete at elevated temperatures (Omer, 2007)

With increases in temperature, the compressive strength of concrete decreases., Fig. 2.8. The specimens were subjected to stress of 40 percent of their compressive strength before the designated temperature was reached. The load was subsequently increased until the specimen failed. The residual strength of silica aggregate containing concrete was almost 50 percent at 1200 ° F, but the substantial decrease began at 800 ° F. In addition, in concrete containing light weight and carbonate aggregate up to 1200 ° F temperature, negligible loss of strength was observed. Lightweight concrete has been found to have greater fire resistance characteristics than normal weight concrete. Temperature increase also greatly affects the Young's modulus of concrete, Fig. 2 .9. With a rise in temperature, the modulus of elasticity for the concrete obtained from various types of aggregates has been found to decrease. In general, because of temperature elevation, the creep and relaxation have also been found to amplify dramatically.

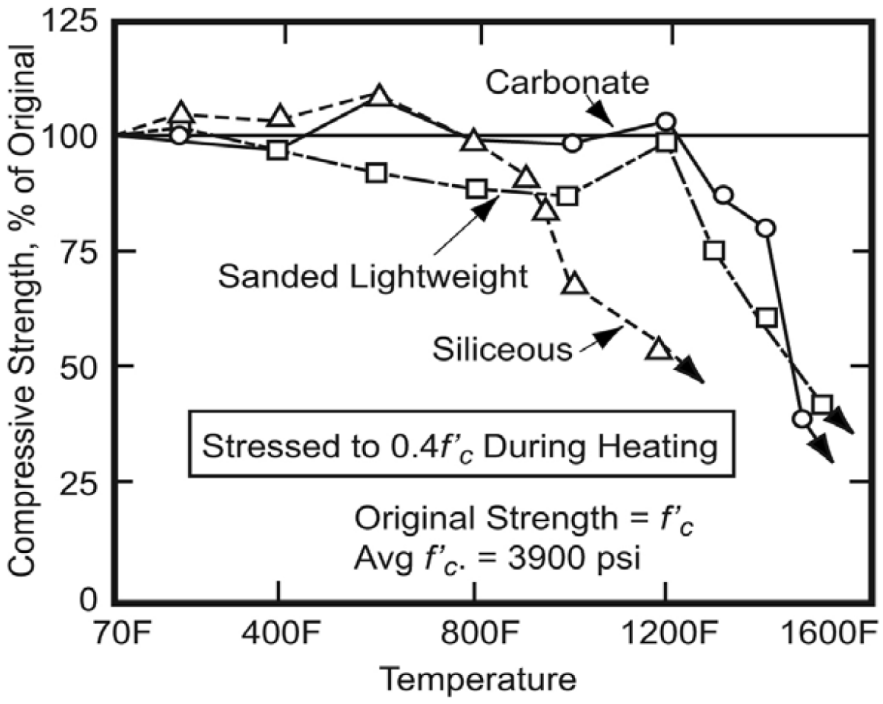

Fig. 2.8 High temperature has a detrimental effect on the strength of concrete (Bilow and Kamara, 2008)

Kodur et al., (2010) observed that concrete loses strength in high temperatures depending on these following conditions:

- Exposure form (percentage of exposure, no. of faces and duration)
- Concrete type (aggregate type, strength etc.)
- Loading (rate of initial load prior to and during fire exposure)

The behaviour of an RC element exposed to fire relies on the following:

- Experiencing internal temperature
- Level of load during burn
- Regime of cooling, cooling rate
- Recovery time of strength after cooling

A thorough review of the experimental data available in the literature will conclude the following. [Lie and Kodur (1995), Abrams (1977), Carvel (2005), Kumar and Kumar (2003), Liu et al. (2010), Ayman (2006), Lie and Irwin (1993) etc.]

- High-strength concrete beams are less fire-resistant than ordinary concrete beams.
- Load level, axial restraints and fire scenario type have a major impact on the total fire efficiency of RC beams.
- HSC has increased strength and stiffness degradation at higher temperatures.
- Load ratio and permeability play an important role in concrete spalling.
- The reduced load level contributes to higher resistance to fire.
- During the heating process, the maximum temperature inside the RC components is not generally found, i.e., the temperature within an element continues to rise for some time even after the temperature of the furnace begins to fall.

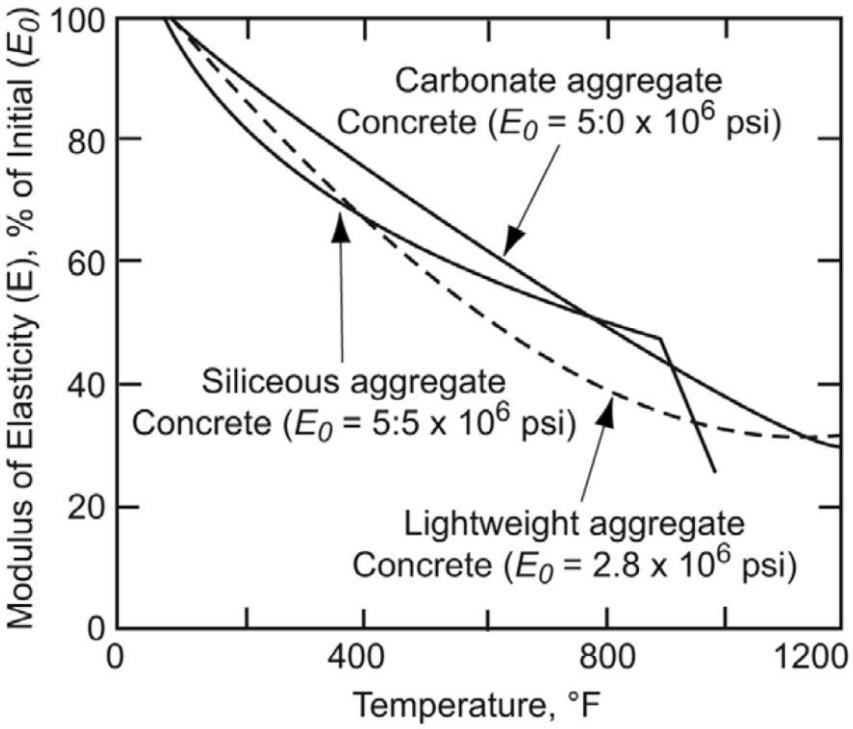

Fig. 2.9 Decreasing the modulus of elasticity of with increasing temperature (Bilow and Kamara, 2008)

Spalling can be considered one of the most dynamic and least understood behaviours of high-temperature concrete (Khoury, 2000). Canisius et al. (2003) suggest that spalling in concrete may occur at 200 °C, not only restricted to higher temperatures. Reinforcement can also be revealed in the case of extreme spalling, resulting in an increased heating rate. It can, therefore, lead to a decrease in the strength of the reinforcement and a deterioration in the mechanical properties of the whole. In addition, due to the reduction in the cross-section, spalling also decreased the structure's strength against imposed loading. Thus, prior to the start of any other fire-induced effect, spalling can affect the overall structure behaviour.

Owing to the evaporation of moisture content, the spalling process consists of high pressure inside the concrete. Therefore, the pressure contributing to spalling starts

to dissipate with the sudden creation of cracks and fragments of concrete. Due to less voids and moisture absorbance capacity, high strength and high-performance concrete are more prone to spalling, Khoury (2000).

The various types of steel bars used as the reinforcement can be divided into different categories, Cadoni et al. (2013 and 2012).

- quenched and self-tempered reinforcement bar (Typically used as main reinforcement)
- cold drawn reinforcement bar (Used as stirrups and/or mesh)
- stainless-steel reinforcement bar (In extreme environmental situations, used)
- hot rolled reinforcement bar (used as rebar)

The quenched and self-tempered rebar is widely used in reinforced structures because of its high strength and effective ductility. The structural steel Weldox 460 E experimental and numerical tests have been documented in literature, (Hopperstad et al., 2003, Børvik et al. 2001,2002,2003). Borvik et al., 2002, considered the content parameters for constitutive modeling in the present research. Hopperstad et al. performed experiments at high strain rates in the Split Hopkinson Tension Bar in 2003 in order to discover the combined effects of strain rate as well as stress triaxiality on Weldox 460 E. They mentioned that with increasing strain rate, the strength of material increases, while on ductility, the effect of strain rate could be considerably determined.

Borvik et al., 2005, conducted experimental investigations of Weldox 460 E steel at high strain rates and elevated temperatures with high stress triaxiality using the Split Hopkinson Tension Bar. The rates of strain ranged from 500 to 1500 s^{-1}, while the temperature ranged from 100 to 500 °C. Compared to quasi-static loading conditions,

the effect of temperature on the stress-strain behavior was important at high strain rates. The curves of engineering stress-strain were derived at various initial temperatures and initial loading conditions with smooth specimens. Initial loading equal to 20 kN has been reported to give a nominal strain rate of between 450 and 550 s^{-1}, while initial loading of 40 kN results in a nominal strain rate of between 1300 and 1400 s^{-1}. The results indicate that mechanical strength as well as elongation decreases with temperature, while strain hardening raises slightly.

Steel strength and stiffness decrease in a manner close to that of concrete under high temperatures. (Freskakis, 1980). Topcu and Karakurt (2008) has concluded that as the deterioration of modulus of elasticity and yield strength of steel bars affects the efficiency of RC structures in fire. The researchers have said that the protective cover thickness should be used to accommodate the fire protection of the RC members. The conventional steel loses one third of its tensile strength at 600 ^{0}C, (Unluoglu et al., 2007). Steel's strength depends on how it is manufactured and the process will influence the quality of the steel itself, (Eurocode-2,2004, Anderberg, 1978, Buchanan, 2001). In 2009, Felicetti et al. confirmed the concept that quenched and self-tempered bars would become more sensitive to elevated temperatures. Elghazouli et al., (2009) conducted a series of experiments on reinforcing steel at normal temperature and under steady and transient extreme temperature conditions. After exposed to elevated temperature ranges the intensity decreases to 10-15 percent in the case of 600 ^{O}C cold-worked bars.

In modeling global behavior and predicting reinforcement fracture at ultimate failure, the bond characteristics between steel reinforcement and concrete are important, (Giroldo and Bailley, 2008). Bingo and Gul (2009), however, studied that the strength

of the bond between concrete and steel increases up to 150 ° C and then decreases with further temperature rise. At elevated temperatures, the yield strength and modulus of elasticity of the steel reinforcement is also recorded to be reduced.

2.5 CRITICAL OBSERVATION

From the literatures, it is found that the subject of nuclear containment under aircraft crash has been studied in the last few decades in order to comprehend the response of nuclear containment structure. The researchers have adopted numerous methods to study the performance against the intentional and accidental crash of the existing containment structures. Over a period of time, the computational modeling and simulation of the issue have been refined.

- Many researchers proposed the reaction force time curve for different aircraft but in every case the target was considered as rigid. In actual scenario, the targets are deformable and the reaction force time curve for deformable target is not available in any literature.
- In most the cases, the response of NPP containment wall has been analysed using reaction force time curve but in very few cases, the geometric model is directly applied on the NPP containment wall.
- There are many types of NPP containment structures in the world. In maximum cases, BWR mark-III containment wall has been used to predict the response of the wall under aircraft crash. Till now the research has not been performed significantly on any other nuclear power plant containment wall.

- The most vulnerable location in BWR containment wall is found to be different in different literature because they have considered very few locations to apply impact load.
- When an aircraft impacts over a target, the extra stress may arise due to induce fire but this scenario has not been considered in any single literature.
- The parametric study on NPP wall under aircraft crash has not been carried out by researcher.

2.6 SCOPE OF PRESENT STUDY

The accurate analysis of nuclear containment wall under high impact load and subsequent developed thermal load due to aircraft crash needs research attention. In the present study the scope of the work is listed below:

1. Study of NPP wall's material (concrete and reinforcement steel) behaviour under high rate of impact loading and subsequent thermal loading at elevated temperature to incorporate the actual material behaviour.
2. Stress and deformation analysis of plain cement concrete (PCC) and reinforcement cement concrete (RCC) flat plate and RCC cylindrical wall due to impact load of aircraft Boeing 707-320, Boeing 767-400, Phantom F4 and Airbus A320 for understanding the structural behaviour of plates.
3. Deformation, stress and damage analysis of real NPP containment wall i.e., Creys-Malville Reactor (CMR), Fessenheim and Bugey Reactor (FBR), Boiling Water Reactor (BWR Mark-III) and Three Mile Island Reactor (TMIR) containment wall under different aircrafts commercial as well as fighter.

4. Determination of most vulnerable location on NPP containment wall (BWR-III) subjected to high impact load due to aircraft crash for proper wall designing and finding the most devasting aircraft with respect to extend of damage.
5. Determination of most damage prone NPP containment wall among CMR, FBR, BWR and TMIR under the impact of Boeing 707-320 aircraft.
6. The deformation behaviour of TMIR containment wall under the impact of Boeing 707-320 aircraft for various parameters i.e., wall thickness, reinforcement ratio, curvature of containment, impact velocities, impact angles and the effect of stain rate
7. Evaluation of reaction force time response curve for Boeing 707-320 aircraft on rigid and non-rigid target with varying curvature and for different impact angles.
8. Characterization of impact load by different approaches i.e., average area approach, geometric model and trifurcation approach and their comparative study in TMIR containment wall.
9. Thermo-coupling analysis of TMIR containment wall subjected to impact of Boeing 707-320 aircraft to observe actual structural behaviour.